J Geod (2011) 85:707–714
DOI 10.1007/s00190-011-0477-8

ORIGINAL ARTICLE

Accuracy assessment of the GPS-TEC calibration constants by means of a simulation technique

Juan Federico Conte · Francisco Azpilicueta · Claudio Brunini

Received: 7 January 2011 / Accepted: 25 April 2011 / Published online: 15 May 2011

Abstract During the last 2 decades, Global Positioning System (GPS) measurements have become a very important data-source for ionospheric studies. However, it is not a direct and easy task to obtain accurate ionospheric information from these measurements because it is necessary to perform a careful estimation of the calibration constants affecting the GPS observations, the so-called differential code biases (DCBs). In this paper, the most common approximations used in several GPS calibration methods, e.g. the La Plata Ionospheric Model (LPIM), are applied to a set of specially computed synthetic slant Total Electron Content datasets to assess the accuracy of the DCB estimation in a global scale scenario. These synthetic datasets were generated using a modified version of the NeQuick model, and have two important features: they show a realistic temporal and spatial behavior and all a-priori DCBs are set to zero by construction. Then, after the application of the calibration method the deviations from zero of the estimated DCBs are direct indicators of the accuracy of the method. To evaluate the effect of the solar activity radiation level the analysis was performed for years 2001 (high solar activity) and 2006 (low solar activity). To take into account seasonal changes of the ionosphere behavior, the analysis was repeated for three consecutive days close to each equinox and solstice of every year. Then, a data package comprising 24 days from approximately 200 IGS permanent stations was processed. In order to avoid unwanted geomagnetic storms effects, the selected days correspond to periods of quiet geomagnetic conditions. The most important results of this work are: i) the estimated DCBs can be affected by errors around ±8 TECu for high solar activity and ±3 TECu for low solar activity; and ii) DCB errors present a systematic behavior depending on the modip coordinate, that is more evident for the positive modip region.

Keywords GPS · Differential Code Biases (DCB) · sTEC · Ionosphere

J. F. Conte (✉) · F. Azpilicueta · C. Brunini
GESA, Facultad de Ciencias Astronómicas y Geofísicas,
Universidad Nacional de La Plata, CONICET,
Paseo del bosque s/n, 1900 La Plata, Argentina
e-mail: fconte@fcaglp.unlp.edu.ar

1 Introduction

The knowledge of the Total Electron Content (TEC) plays a key role in the study of the ionosphere. It is defined as the integral of the electron density along a given ray path and is proportional to the number of free electrons contained in a cylinder whose longitudinal axis is the ray path and whose cross-section is 1 m^2. This parameter can be estimated from a variety of different techniques and instruments, being outstanding the satellite altimetry missions (TOPEX/Poseidon, Jason1, etc.) (Fu et al. 1994), and the Global Positioning System (GPS). Other instruments that are not discussed in this work but provide information on TEC include the Russian Global Navigation Satellite System (GLONASS) (Jakowski et al. 2002) and the DORIS International Service (Willis et al. 2010).

Global Positioning System measurements provided by GPS permanent stations are already well established as a powerful, accessible and precise tool for ionospheric remote sensing (Brunini et al. 2004; Hernández-Pajares et al. 2009). Nevertheless, there are some calibration constants that must be estimated and eliminated when retrieving slant Total Electron Content (sTEC) values from GPS signals (the sTEC is defined as the integral of the electron density along the satellite to the receiver line of sight). These calibration constants are the so-called receiver and satellite differential code biases (DCBs) and cannot be neglected since they

usually represent equivalent values of up to 40 TEC units $\left(1\ \text{TECu} = 10^{16}\,\text{m}^{-2}\right)$ for the receiver and 20 TECu for the satellite, respectively. Subsequently, in the computation of the sTEC between a receiver and a satellite, the combination of both DCBs can give values as high as 100 TECu in many cases (Sardon et al. 1994; Brunini and Azpilicueta 2010).

The DCBs, as well as the bias in the carrier-phase measurements (the so-called Inter-Frequency Biases, IFB), are mainly introduced by the satellite and receiver hardware and firmware. The basic principle of GPS measurements is to measure, as accurately as possible, the time interval that the signal transmitted by the satellite needs to reach the receiver. Every electronic device, including GPS satellites and receivers, has a time response (delay) that depends on the frequency and broadband of the signal. Clearly, these time responses introduce time-dependent delays on every GPS observable that need to be estimated and removed, if accurate GPS sTEC values are required. For further information see Sardon et al. (1994), Schaer (1999) and Brunini and Azpilicueta (2009).

Global Positioning System ionospheric sounding is based on measurements of the carrier-phase shift and the code-delay on the two GPS L-band frequencies ($f_1 = 1{,}575.42$ MHz, and $f_2 = 1{,}227.60$ MHz). The carrier-phase measurements are identified as L_1 and L_2, and the corresponding code-delay as P_1 and P_2. The GPS ionospheric observable on the carrier-phase is defined by $L_4 = L_1 - L_2$, and on the code-delay by $P_4 = P_2 - P_1$ (assuming all quantities in corresponding units).

As it is well known, the code-delay observations are much more affected by the observational noise and the multi-path effects (around 2 orders of magnitude) than the carrier-phase observations, but they are not affected by the ambiguity terms. Therefore, in order to overcome the problem of the ambiguity term, the so-called carrier-to-code leveling technique is applied. This technique is a commonly used procedure to eliminate the carrier-phase ambiguity term from the GPS carrier-phase ionospheric observable (Schaer 1999). Leveling the carrier-phase to the code-delay ionospheric observable consists of shifting every continuous arc of the carrier-phase ionospheric observable by an appropriate constant value (leveling constant) that makes the carrier-phase data match (on average) the noisier, but unambiguous code-delay data. Those constant values are interpreted as the carrier-phase ambiguity terms on the carrier-phase ionospheric observable. This procedure has the advantage of eliminating the ambiguity terms from the carrier-phase observations, at the expense of introducing the DCBs. For details on this procedure see Brunini (1998) or Azpilicueta et al. (2006).

The ionospheric observable obtained after applying the carrier-to-code leveling procedure is usually denoted by $\tilde{L}4$, and is related to the sTEC by the following equation (assuming all quantities given in TECu)

$$\tilde{L}4 = \text{sTEC} + B_{\text{R}} + B^{\text{s}} + \varepsilon_{\text{L}} \tag{1}$$

where B_{R} represents the DCB for receiver R and B^{s} the DCB for satellite S. The ε_{L} is the combination of the observational noise, multi-path effects on the carrier-phase observations and any additional error due to the leveling procedure.

It comes out from Eq. (1) that the DCB terms have to be carefully estimated and removed from the $\tilde{L}4$ observable in order to obtain an accurate estimation of the sTEC. A usual procedure is to assume the DCBs as constants for a given period of time (1 day in this work) and to estimate them from the GPS raw data, along with the sTEC (Sardon et al. 1994; Azpilicueta et al. 2006; Hernández-Pajares et al. 2009).

Brunini and Azpilicueta (2009) and Brunini and Azpilicueta (2010) presented a method for assessing the accuracy of the DCBs estimation. It consists on the generation of a synthetic sTEC dataset that is realistic and free of DCBs (in other words, all DCBs are set to zero by construction). Then, this dataset is processed and calibrated with a standard calibration technique, obtaining a set of estimated values for the DCBs. The dispersions of these values indicate the accuracy of the obtained sTEC. In the works mentioned before the authors applied the method to assess the accuracy of the estimated DCBs when a station-by-station calibration algorithm was used for equatorial, mid and high geomagnetic latitude stations. The main objective of this paper is to apply the same method for assessing the accuracy of the estimated DCBs when a global adjustment is performed, i.e. when the satellite DCB and the receiver DCB of a global GPS network are estimated all together at the same time (Hernández-Pajares et al. 2009). About 200 GPS stations were considered in this research.

For the purpose of understanding the effect of the 11-year cycle of the solar radiation, two scenarios were considered corresponding to years 2001 (high solar activity) and 2006 (low solar activity), both under quiet geomagnetic conditions. To fulfill this objective, only days presenting an average Dst index higher than −25 nT were selected, according to the values published at http://wdc.kugi.kyoto-u.ac.jp/dstdir/. Following Gonzalez et al. (1994), a geomagnetic storm can be defined as an interval of time when a sufficiently intense and long-lasting interplanetary convection electric field leads to an intensified ring current sufficiently strong to exceed some key threshold of the quantifying storm Dst index. Consequently, this increase in the electro-magnetic activity produces unpredictable and very complicated fluctuations in the electron content of the ionosphere. Therefore, since every ionospheric model makes assumptions and approximations in order to simplify the ionosphere's physics, most modeled predictions of the ionospheric behavior under geomagnetic storms conditions will fail to represent a realistic ionosphere. This is the main reason why only days

under quiet geomagnetic conditions have been selected for this research.

In order to assess the influence of seasonal changes in the ionospheric behavior, three consecutive days for each equinox and solstice epochs were considered.

2 Computation of the synthetic datasets

2.1 Description of the technique

This research relies on a specially developed technique (Brunini and Azpilicueta 2009) used to generate synthetic datasets that are realistic, except that all calibration constants are set to zero. The technique uses the NeQuick model (Radicella and Leitinger 2001) with a series of modifications in the manner of computing the critical frequency, f_0F2, of the F2 layer (Brunini et al. 2009).

The NeQuick model allows computing the electron density distribution, $N_e(\varphi, \lambda, H, t, S_f)$, as a function of the geographic latitude and longitude, φ and λ, the height above the surface of the Earth, H, the Universal Time, t, and the equivalent solar flux level, S_f (Nava et al. 2005). The equivalent solar flux level is the main driver of the NeQuick model, so that given a S_f value, the electron density space and time variations are controlled by the ITU-R coefficients, which determine the values of the F2-layer parameters (the electron density and height of the F2 peak) and then define the shape of the NeQuick vertical profile. Mostly due to this dependence on the ITU-R parameters, the spatial and time variations of the electron concentration computed with the NeQuick model, and hence the resulting sTEC, are often smoother than the actual ones (Nava et al. 2005). In the standard formulation of NeQuick, the S_f for a particular day is mainly determined by the $F10.7$ index, which measures the solar radiation at a wavelength of 10.7 cm. This index acts as a proxy of the extreme ultra-violet (EUV) radiation which is the main ionization driver. In order to improve the geographic and temporal resolution of the NeQuick, a data assimilation technique was applied. The technique, which is documented in Brunini and Azpilicueta (2009), is a modification of the one developed by Nava et al. (2005). It consists on using GPS sTEC determinations previously calibrated to estimate S_f values every certain period of time. In Nava et al. (2005) global grids of GPS vTEC determinations (known as Global Ionospheric Maps, GIMs) are used to estimate a S_f value per hour, and then the S_f values for the required period of time are computed through linear interpolation. In the present work we used GPS sTEC determinations to directly estimate a S_f value every 5 min. This modification gives the model more flexibility to represent the actual state of the electron density. Finally, the obtained S_f series were used to compute the synthetic sTEC dataset.

The sTEC values calculated with the modified version of NeQuick fulfill the three basic requirements: i) provide a realistic representation of the actual state and rate of change of the ionospheric sTEC; ii) to be free from DCBs (or equivalently, all DCBs are equal to zero); and iii) to be free from measurements, multipath and leveling errors, i.e. $\varepsilon_L = 0$ in Eq. (1).

2.2 Characteristics of the scenarios

The technique presented in Sect. 2.1 was applied to a network of approximately 200 simulated stations with identical location to the ones already existing within the IGS global network (Dow et al. 2009). As was mentioned in Sect. 1, 12 days were analyzed for year 2001 (high solar activity) and 12 days for year 2006 (low solar activity). To avoid unwanted effects due to geomagnetic storms, the daily mean Dst index values were greater than −25 nT. Table 1 presents the dates for days analyzed.

3 Accuracy assessment techniques

3.1 Global LPIM calibration strategy

The La Plata Ionospheric Model (LPIM) (Azpilicueta et al. 2006) was used to calibrate the synthetic datasets created with the modified version of the NeQuick Model. The calibration process of the LPIM, like in most GPS computation techniques, begins after the $\tilde{L}4$ values are obtained from the GPS raw data files (see Sect. 1). To obtain a global distribution of the vertical Total Electron Content (vTEC), the ionosphere is represented by the so-called thin-layer model. This model approximates the whole ionosphere with a spherical shell of infinitesimal thickness located at a given effective height, H, above the surface of the Earth. For this work a value of 350 km was adopted. The point where the receiver to the satellite line of sight pierces the shell is called the ionospheric

Table 1 Summary of the days considered in this research

Epoch	Days of year, 2001	Days of year, 2006
March equinox	66–68 (−7)	60–62 (2)
	[7–9]	[1–3]
June solstice	154–156 (−4)	171 – 173 (−2)
	[3–5]	[20–22]
September equinox	244–246 (−7)	254–256 (−7)
	[1–3]	[11–13]
December solstice	340–342 (−19)	340–342 (−6)
	[6–8]	[6–8]

The average Dst index for each group of three consecutive days is given in parentheses. Also, the corresponding calendar dates are given in brackets

piercing point (IPP). Once the IPP is defined, it is necessary to introduce a mapping function to relate the sTEC and the vertical Total Electron Content (vTEC at the IPP, defined as the integral of the electron density along the vertical line that passes through the IPP). Several approximations are generally used for this mapping function, but in this research, the simplest one has been used as given by:

$$\frac{\text{vTEC}}{\text{sTEC}} = \cos(z) = \sqrt{1 - \left(\frac{R}{R+H}\right)^2 \sin^2(z')}. \quad (2)$$

In this expression z' is zenith angle of the satellite at the receiver; R is the mean Earth's radius; and z is the zenith angle at the IPP.

As a second step, a suitable mathematical representation of the spatial and temporal variability of the vTEC has to be chosen. Since the purpose of this research is to work at a global scale, a truncated spherical harmonic expansion dependent on the IPP coordinates (a modip sun-fixed coordinate system is adopted) (Azpilicueta et al. 2006) was used to represent the spatial variability. The temporal variability was introduced through a stepwise function dependent on the Universal Time (UT) for the spherical harmonic coefficients. In that case, the mathematical expression obtained is

$$\text{vTEC}(\mu, h, t) = \sum_{l=0}^{L} \sum_{m=0}^{l} \left(a_{lm}(t) \cos\left(2\pi \frac{mh}{24}\right) + b_{lm}(t) \sin\left(2\pi \frac{mh}{24}\right) \right) P_{lm}(\sin(\mu)) \quad (3)$$

where t is the universal time, h is the hour angle ($h = t + \lambda_{\text{IPP}} - 12$); μ is the modip latitude, firstly proposed by Rawer (1984) and defined as

$$\mu = \text{arctg}\left(\frac{I}{\sqrt{\cos(\varphi)}}\right),$$

where I is the true magnetic dip, usually at a height of 350 km, and φ is the geographical latitude; $a_{lm}(t)$ and $b_{lm}(t)$ are the time dependent-coefficients (mathematically represented by a stepwise function with a refreshing interval of 1 h); L is the maximum degree of the expansion (15 for this work); and P_{lm} is the associated Legendre function.

Finally, introducing Eqs. (2) and (3) into Eq. (1) leads to the key expression for this research:

$$\tilde{L}4 = M(z) \cdot \text{vTEC}(a_{lm}, b_{lm}) + B_{\text{R}} + B^{\text{s}} + \varepsilon_{\text{L}}, \quad (4)$$

where $M(z)$ is the inverse of the mapping function given by Eq. (2).

Differential code biases for each satellite and receiver and one set of spherical harmonic coefficients per hour (more than 6,000 coefficients per day) were simultaneously estimated using the Least Squares Method.

3.2 Accuracy assessment

By construction, the synthetic sTEC datasets are free of calibration constants, which is equivalent to saying that if the synthetic datasets were processed as real data, the obtained DCBs should all be zero. But as the calibration technique involves several approximations, the resulting DCBs would not be zero and the order of magnitude of them could help to quantify the level of accuracy of the calibration process. Hereafter, the designation "DCB errors" will be used instead of "estimated DCBs".

4 Results and discussions

The LPIM calibration procedure, described in Sect. 3.1, was applied to the synthetic sTEC datasets, thus obtaining 24 sets of hourly spherical harmonic coefficients per day and the daily "DCB errors" for every receiver and satellite. By applying the error propagation law, LPIM also computed the standard deviation for every estimated coefficient and "DCB error".

To accomplish the objectives of this research, the "DCB errors" and their corresponding standard deviations were analyzed, specifically in relation to the geographical distribution of the GPS receivers. It is worth mentioning that the "DCB errors" of the satellites were discarded because their values were at least ten times smaller than those corresponding to the receivers; hence the following analysis and discussions only focus on the "DCB errors" of the receivers.

As was mentioned in Sect. 3.1, LPIM implements a series of approximations (the thin-layer ionospheric model, the mapping function and the truncated spherical harmonic expansion), and because the ionosphere has a clear and distinctive latitudinal pattern, it was expected then that the "DCB errors" would present some systematic behavior when plotted against a latitudinal coordinate. So, in order to corroborate (or discard) this concept, plots of "DCB errors" against modip latitude were made for every year and every epoch considered (comprising three consecutive days with the same GPS stations for the three days). Figure 1 presents the four plots for the year 2001 and Fig. 2, the plots corresponding to the year 2006.

4.1 Positive modip region

The most distinguishing characteristic of the set of eight plots is a clear systematic behavior of the "DCB errors" for the region of positive values of modip. In six of the eight plots, it can easily be seen that an almost straight line (with positive slope) ascends from the modip equator towards the modip

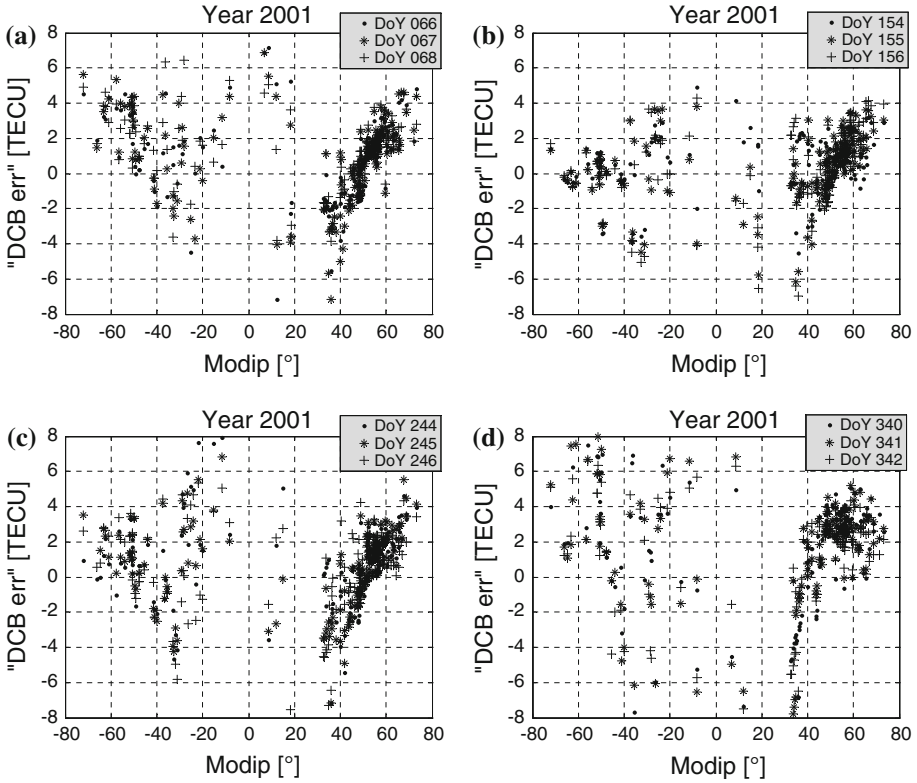

Fig. 1 Series of four plots of "DCB error" [TECu] against modip [°] for the periods of 2001. The corresponding calendar dates are: **a** March 7–9, **b** June 3–5, **c** September 1–3, **d** December 6–8. Each *plot* represents the latitudinal behavior of "DCB error" for a period of three consecutive days

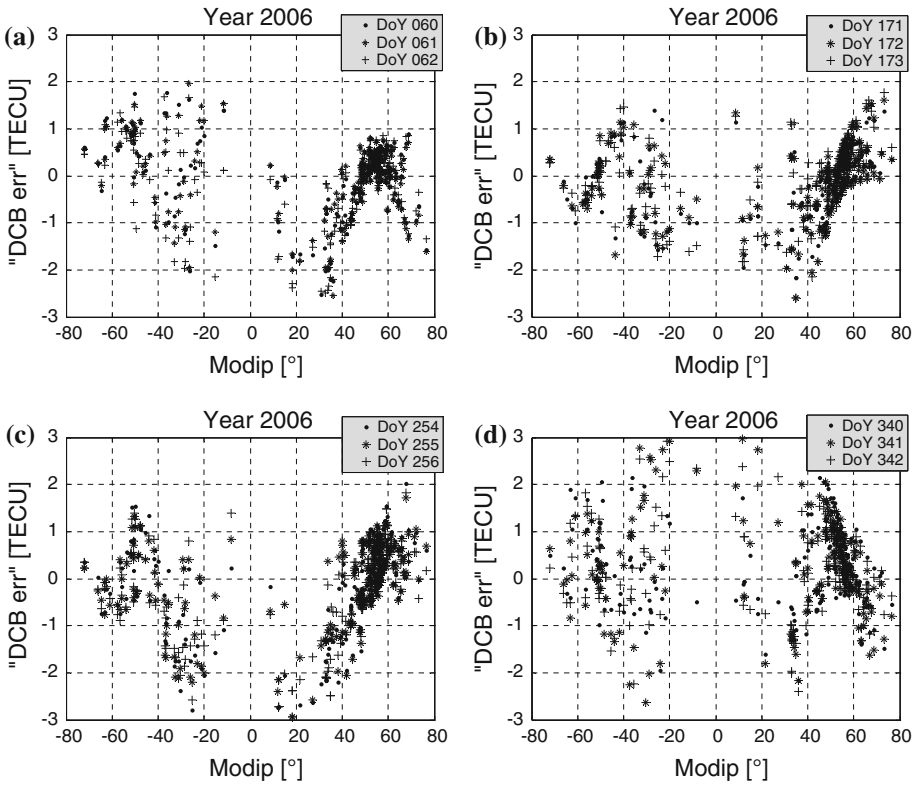

Fig. 2 Series of four plots of "DCB error" [TECu] against modip [°] for the periods of 2006. The corresponding calendar dates are: **a** March 1–3, **b** June 20–22, **c** September 11–13, **d** December 6–8. Each *plot* represents the latitudinal behavior of "DCB error" for a period of three consecutive days

"north pole", in opposition to the latitudinal behavior of TEC. For the Fig. 2a, d the behavior is not so clear, but systematic anyway. The "DCB errors" for year 2001 reach maximum values of ±8 TECu, and ±3 TECu for year 2006, in a direct relationship with the corresponding period of the solar cycle of 11 years. In other words, during high solar activity periods,

the accuracy in the DCB estimation is bounded by ±8 TECu, while during low solar activity periods is bounded by ±3 TECu. This shows that the expected accuracy for the GPS sTEC degrades as the solar activity increases.

At this point, it is of importance to remark that since the "DCB errors" are not the actual errors but an accuracy assessment of the estimated DCBs based on realistic although simulated sTEC values, the absolute quantities mentioned in the last paragraph (8 and 3 TECu) represent the lower bound one would expect for the actual errors present in the estimated DCBs.

4.2 Negative modip region

The behavior in the region of negative modip is quite different. Except for the Fig. 2c in which an approximately straight line with negative slope descending from the modip "south pole" towards the modip equator can be seen, the rest of the plots present no clear systematic behavior as a function of modip. In other words, for negative modip the "DCB errors" values are much more dispersed. The "DCB error" magnitudes obtained for negative modip are, on average, similar to those corresponding to positive values of modip.

The reasons behind the systematic behavior observed for positive modip are the approximations LPIM implements, specially the mapping function. The mapping function used in this work depends on the height of the single layer and on the angle between the receiver to the satellite line of sight and the vertical line that passes through the IPP, z. This only dependence on the z coordinate implies that the ionosphere has an azimuthal symmetry, and in turn this non-realistic approximation could lead to errors in the calibration constants. On the other hand, the assumption of a constant height for the single layer model is also an approximation that introduces errors due to the fact that the altitude of the F2 peak is not the same for different regions of the terrestrial ionosphere and also changes along the day and the year.

The behavior of the "DCB errors" in the negative modip region is of particular interest, because in principle it would be expected to show systematic patterns as those observed in positive modip regions, since all the approximations that LPIM uses are symmetric with respect to the modip equator. However and as was previously explained, the general behavior for the negative modip region is significantly different, with no apparent systematism and presenting a much more scattered distribution. Two possible explanations were analyzed to try to understand this particular behavior: i) the scarce distribution of GPS receivers in the southern hemisphere (approximately 70% of the IGS GPS receivers are located in the northern hemisphere) and ii) the fact that the southern hemisphere's ionosphere is more complicated to model. It has to be clear that the second possible explanation presented in the last sentence refers to the fact that all the approximations taken into account by the models mentioned in this paper are limited to represent the complexity of the southern hemisphere's ionosphere.

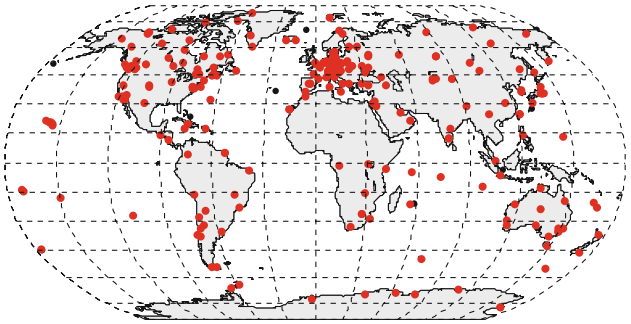

Fig. 3 Global distribution of the GPS permanent stations used in this work

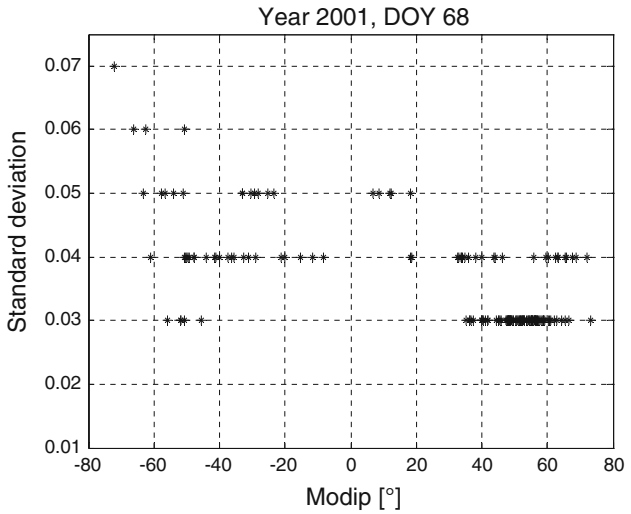

Fig. 4 Plot of the standard deviations for the "DCB errors" (normalized to the standard deviation of the unity of weight) obtained after LS fitting versus modip [°] for DoY 68 (March 9) of 2001. The levels of discretization observed are due to the fact that LPIM rounds off the standard deviation values at two decimals

From Fig. 3 it is clear that GPS stations are sparsely distributed in the southern hemisphere, and then more dispersion is expected for those quantities estimated for negative modip, because when a data sample is not well distributed worst errors congregate to regions with poor data coverage. Therefore, in order to determine the degree of influence of the data samples on the scattered distribution of "DCB errors" for negative modip, plots of their standard deviation against modip were analyzed. Hence, a plot of the standard deviations of the "DCB errors" against the modip latitude of the stations was made for each one of the 24 days considered. Every plot presented the same pattern as the one depicted in Fig. 4, showing that most of the highest values of standard deviation (normalized to the standard deviation of the unity of weight) correspond to GPS stations with negative modip.

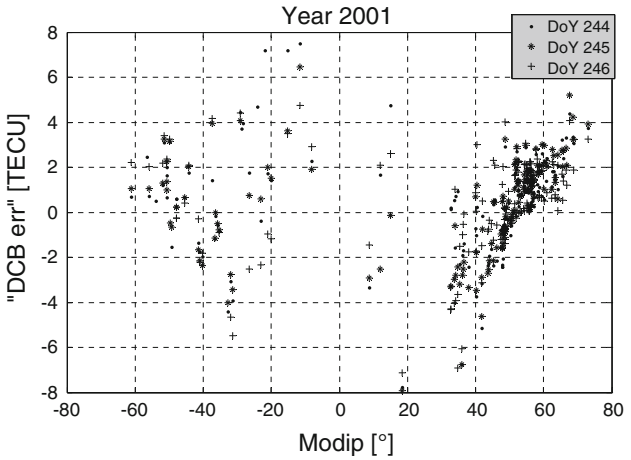

Fig. 5 Representative plot of "DCB error" [TECu] versus modip [°] similar to those of Fig. 1, but with the difference that here those "DCB errors" presenting the highest values of standard deviation were eliminated

This clearly indicates that the distribution of the data samples has some influence on the scattered distribution of the "DCB errors" for negative modip.

However, the effect is small, as can be seen from Fig. 5. In this figure a plot similar to those depicted in Fig. 1 is presented, but this time without the "DCB error" values with the highest standard deviation (similar plots that are not presented in this paper were obtained for the remaining days). A dispersed pattern can also be appreciated for negative modip, indicating that some influence of the data samples exists but that it is not strong enough to explain the scattered distribution of "DCB errors" observed for negative modip. It is worth mentioning that the standard deviation of the "DCB errors" normalized to the standard deviation of the unity of weight has no information on the physics of the ionosphere; it only contains information about the data samples geographic distribution and the mathematics of the calculation.

Even though the analysis of the standard deviations against the modip latitude of the GPS stations represents a direct way to understand the degree of influence the data samples have on the scattered distribution of "DCB errors" for negative modip locations, another experiment was conducted to definitively determine the main responsible for the behavior observed in negative modip locations. It consisted on the calculation of a synthetic sTEC dataset for approximately 320 simulated stations more homogeneously distributed, and even more important, with a more symmetrical distribution with respect to the modip equator (see Fig. 6). Then, this dataset was calibrated with the LPIM model and again, the "DCB errors" obtained after the calibration process were analyzed against the modip latitude. The three consecutive days corresponding to the 2001 September equinox were selected because they represent one of the worst-case scenarios when the standard deviations of the "DCB errors" are taken into consideration.

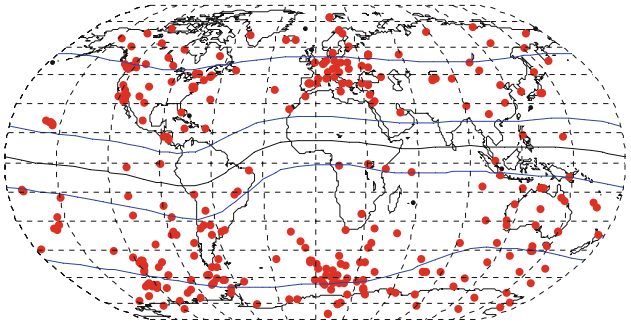

Fig. 6 Geographical distribution of the approximately 320 simulated GPS stations. Also, the modip equator (*black curve*) and some modip isolines (*blue curves*) are represented

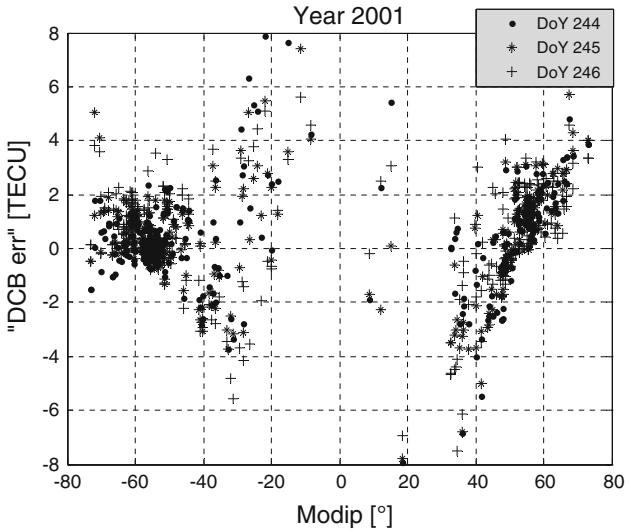

Fig. 7 Representative plot of "DCB error" [TECu] versus modip [°] similar to that of Fig. 1c, but with the difference that here the "DCB errors" correspond to the simulated stations presented in Fig. 6

The results are presented in Fig. 7. In this figure, it can clearly be seen that the behavior for both positive and negative modip locations is the same as the one observed in Fig. 1c. Particularly, the dispersed pattern is still present and continues dominating the distribution of "DCB errors" for negative modip.

Then, after the analysis presented in the preceding paragraphs the results indicate that the second hypothetical error source dominates in the calibration process. The complex physics of the ionospheric southern hemisphere, particularly over the South American region (and hence the difficulties of the ionospheric models to predict it) might be the responsible for the dispersion observed for the "DCB errors" for negative modip. This statement could be supported by several investigations which demonstrate that the ionosphere corresponding to negative modip is more difficult to model, since its physics is more complex and unpredictable (for example see Abdu et al. 2005).

Finally, another important fact to highlight is the apparent lack of symmetry between equinoxes for both years, although it is more evident for the year 2006. Comparing Figs. 1a, c, and 2a, c this asymmetry can easily be seen. It is reasonable to expect an almost symmetric behavior between equinoxes, since the principal ionization factor driving the electron content of the ionosphere is the Sun's EUV and X-ray radiation, and during equinoxes the Sun is in the same apparent position with respect to the Earth. However, Azpilicueta et al. (2011) demonstrated that the annual pattern of the mean global TEC presents an approximately symmetric behavior for days of the year (DoY) 80—March 21 (very close to DoY 81, the March equinox) and 305—November 1 (39 days later than the September equinox), suggesting that the direct association of the semi-annual anomaly with the equinoxes is only an approximation (the semi-annual anomaly produces global mean TEC values larger for equinoxes than for solstices). Therefore, this similarity of the mean global TEC between DoY 80 and 305 (instead of the equinox days of March and September) could be the explanation for the aforementioned lack of symmetry.

5 Summary

By means of a technique that involves the utilization of a synthetic sTEC dataset, it has been demonstrated that for any ordinary day under quiet geomagnetic conditions, the approximations made by most of the sTEC calibration techniques based on GPS observations (like the LPIM), have an impact on the magnitudes and the behavior of the obtained calibration constants. For stations located in the region of positive modip, the "DCB errors" (quantities that represent an accuracy assessment of the estimated DCBs) have a systematic behavior that compensates the latitudinal variability of TEC. This behavior is observed for both high and low solar activity periods, with differences only in the magnitudes involved (± 8 TECu for high solar activity and ± 3 TECu for low solar activity).

Possible explanations have also been outlined for the scattered behavior observed for negative modip locations, concluding that the data samples distributions have a small effect and that the most probable cause responsible for that behavior is the complex physics of the southern ionosphere.

Acknowledgments The authors thank Prof. Pascal Willis and the reviewers of the manuscript for their insightful suggestions and comments that have enhanced the quality of our work.

References

Abdu MA, Batista IS, Carrasco AJ, Brum CGM (2005) South Atlantic magnetic anomaly ionization: a review and a new focus on electrodynamic effects in the equatorial ionosphere. J Atmos Solar Terrestr Phys 67:1643–1657. doi:10.1016/j.jastp.2005.01.014

Azpilicueta F, Brunini C, Radicella SM (2006) Global ionospheric maps from GPS observations using modip latitude. Adv Space Res 38(11):2324–2331. doi:10.1016/j.asr.2005.07.069

Azpilicueta F, Brunini C, Radicella SM (2011) Semi-annual anomaly and annual asymmetry on TOPEX TEC during a full solar cycle. In: Proceedings of 2009 IAG Symposium, international association of Geodesy symposia series 136. ISBN: 978-3-642-20337-4

Brunini C (1998) Global Ionospheric Model from GPS measurements. Doctoral thesis, Facultad de Ciencias Astronómicas y Geofísicas, UNLP. La Plata, Argentina

Brunini C, Azpilicueta F (2009) Accuracy assessment of the GPS-based slant total electron content. J Geod 83:773–785. doi:10.1007/s00190-008-0296-8

Brunini C, Azpilicueta F (2010) GPS slant total electron content accuracy using single layer model under different geomagnetic regions and ionospheric conditions. J Geod 84:293–304. doi:10.1007/s00190-010-0367-5

Brunini C, Meza A, Azpilicueta F, Van Zele M, Gende M, Díaz A (2004) A new ionosphere monitoring technology based on GPS. Astrophys Space Sci 290:415–429

Brunini C, Azpilicueta F, Gende M, Aragón-Ángel A, Hernández-Pajares M, Juan JM, Sanz J (2009) Toward a SIRGAS service for mapping the ionosphere's electron density distribution. Submitted to IAG symposia series, Springer, Berlin

Dow JM, Neilan RE, Rizos C (2009) The international GNSS Service in a changing landscape of global navigation satellite systems. J Geod 83(3-4):191–198. doi:10.1007/s00190-008-0300-3

Fu LL, Christensen E, Yamarone C, Lefebvre M, Menard Y, Dorrer M, Escudier P (1994) TOPEX/POSEIDON mission overview. J Geophys Res 99(C12) 24:369–381

Gonzalez WD, Joselyn JA, Kamide Y, Kroehl HW, Rostoker G, Tsurutani BT, Vasyliunas VM (1994) What is a geomagnetic storm? J Geophys Res 99(A4):5771–5792. doi:10.1029/93JA02867

Hernández-Pajares M, Juan JM, Sanz J, Orus R, García-Rigo A, Feltens J, Komjathy A, Schaer SC, Krankowski A (2009) The IGS VTEC maps: a reliable source of ionospheric information since 1998. J Geod 83(A4):263–275. doi:10.1007/s00190-008-0266-1

Jakowski N, Heise S, Wehrenpfennig A, Schluter S, Reimer R (2002) GPS/GLONASS-based TEC measurements, as a contributor for space weather forecast. J Atmos Solar Terrestr Phys 64(5–6):729–735. doi:10.1016/S1364-6826(02)00034-2

Nava B, Coïsson P, Miró Amante G, Azpilicueta F, Radicella SM (2005) A model assisted ionospheric electron density reconstruction method based on vertical TEC data ingestion. Ann Geophys 48(2):313–320

Radicella SM, Leitinger R (2001) The evolution of the DGR approach to model electron density profiles. Adv Space Res 27(1):35–40. doi:10.1016/S0273-1177(00)00138-1

Rawer K (ed) (1984) Encyclopedia of physics, geophysics III: part VII. Springer, Berlin pp 389–391

Sardon E, Rius A, Zarraoa N (1994) Estimation of the transmitter and receiver differential biases and the ionospheric total electron content from global positioning system observations. Radio Sci 29:577–586. doi:10.1029/94RS00449

Schaer S (1999) Mapping and predicting the earth's ionosphere using the global positioning system. PhD thesis, Bern University, Bern, Switzerland

Willis P, Fagard H, Ferrage P, Lemoine F, Noll CE, Noomen R, Otten M, Ries JC, Rothacher M, Soudarin L, Tavernier G, Valette JJ (2010) The international DORIS service, steps toward maturity. Adv Space Res 45(12):1408–1420. doi:10.1016/j.asr.2009.11.018